IEEE Transactions on Nuclear Science, Vol. NS-30, No. 4, August 1983

DESIGN, CONSTRUCTION AND PERFORMANCE OF THE INS RFQ LINAC 'LITL'

N. Ueda, T. Nakanishi, S. Arai, T. Hattori, T. Fukushima, Y. Sakurada, T. Honma,
N. Tokuda, S. Yamada, M. Takanaka, A. Itano*, A. Mizobuchi and Y. Hirao
Institute for Nuclear Study, University of Tokyo
Tanashi, Tokyo 188, Japan

Summary

An RFQ linac 'LITL' (Lithium Ion Test Linac) was constructed and accelerated ion beams of H^+, H_2^+, H_3^+, $^3He^+$, $^6Li^+$ and $^7Li^+$. The machine was designed to accelerate particles with charge to mass ratio (q/A) of 1 ∿ 1/7 injected at 5 keV/u up to 138 keV/u. The acceleration cavity of four vane structure is 56 cm in diameter and 138 cm in length. Transmission exceeding 90 % has been obtained for proton beam of 80 μA. The acceleration characteristics agree well with the computer simulation with PARMTEQ. For the acceleration of $^7Li^+$, an rf power of 22 kW is fed with a loop coupler. In cw operation, an electric field of 205 kV/cm has been applied, which is required for $^7Li^+$ acceleration and corresponds to 1.8 times the Kilpatrick's criterion. A maximum field of 2.0 times the criterion has been achieved, in pulse operation, with a duration width of 5 ms and repetition period of 25 ms. Operation of the machine is easy and stable.

Introduction

It has been shown that RFQ linac is an effective accelerating structure for high intensity beam at low energy region.[1,2] It is also preferable as a lowest stage of a heavy ion accelerator system for its acceptability of low velocity beam and bunching function. On application of RFQ for heavy ions, however, should be studied several subjects on the beam dynamics design, machine structure and rf system: (1) What choice of RFQ parameters gives large acceptance and high accelerating rate. (2) What structure and rf system are good for heavy ions which have wide ranges of charge to mass ration and of beam intensity.

In order to study these subjects, beam dynamics study and model study were made.[3,4] On the basis of the studies, a four vane structure driven with a loop coupler was chosen. The operation frequency was chosen at 100 MHz which gives a reasonable acceptance and accelerating rate for heavy ions with medium mass number.

Table 1. Parameters of the INS RFQ Linac LITL

Ion	q/A = 1 ∿ 1/7
Injection Energy	5 keV/u
Output Energy	138 keV/u
Operating Frequency	100 MHz
Normalized Emittance at Input	0.6 π mm·mrad
Vane Length	122.3 cm
No. of Cells	132
Characteristic Bore Radius, r_0	0.41 cm
Minimum Bore Radius	0.25 cm
Focusing Strength, B_0	5.0
Maximum Defocusing Strength, Δ_b	-0.11
Intervane Voltage	62 kV (q/A = 1/7)
Maximum Field	205 kV/cm
Transmission (q/A = 1/7)	94 % (0 mA)
	92 % (2 mA)
	64 % (10 mA)

* National Institute of Radiological Sciences, Anagawa, Chiba 260, Japan.

Beam Dynamics Design

Considering ion sources and related power supplies available at INS, the input beam parameters were chosen as follows; q/A = 1 ∿ 1/7 ($H^+, \cdots, Li^+, N_2^+, \cdots$), the injection energy T_{inj} = 5 keV/u, and the normalized emittance ε_N = 0.6 π mm·mrad. The maximum surface field strength of 205 kV/cm was supposed to be applicable, which corresponds to 1.8 times the Kilpatrick's criterion at 100 MHz. Under these conditions optimum vane parameters were searched to higher accelerating rate and transmission. The characteristic radius (r_0) is set constant. A couple of new formulations have been introduced at the design. One is of radial matching.[5] The other is of rapid bunching of input dc beam.[6] A computer program GENRFQ was coded to determine the vane parameters.[6] Detailed description on the beam dynamics design is given in another paper.[7] In Table 1, the parameters of LITL are given. In Fig. 1, the vane parameters vs. cell number are shown.

Radial Matching Section The electric field potential in the radial matching section is expanded in a Fourier-Bessel series, and the lowest term was adopted. Then the potential is expressed as

$$U(r, \psi, z) = \frac{V}{2} \frac{I_2(kr)}{I_2(ka)} \sin kz \cos 2\psi \quad ,$$

where a is a bore radius at the end of the radial matching section, $k = \pi/2\ell$ and ℓ is the length of the section. It leads to a focusing strength increasing along the beam axis as

$$B(z) = B_0 \sin kz \quad .$$

With this formalism, the overlap between the input beam phase ellipse and the time dependent RFQ acceptance was calculated at higher than 90 %. At LITL the length has been set at 6 βλ, or 12 cells.

Rapid Bunching of an Input DC Beam Rapid bunching is accomplished in a section named prebuncher, where separatrix area is kept constant and the synchronous phase is increased to -60° within a half period of the small longitudinal phase oscillation. This method is efficient for a low intensity beam.

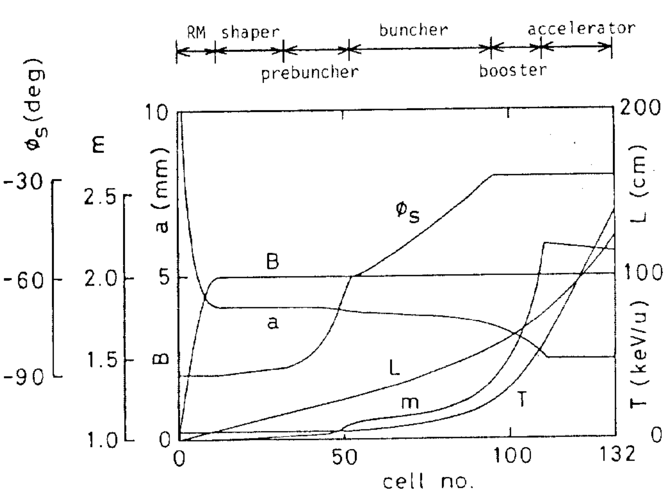

Fig. 1. The vane parameters of LITL vs. cell number.

0018-9499/83/0800-2975$01.00

Acceleration Cavity

Structure

The cavity cross section at the quadrupole symmetry plane was determined with SUPERFISH so that the resonant frequency is 100 MHz for the TE210 mode. The cavity is 56 cm in diameter and 138 cm in length. The vanes are 122.3 cm in length and are set with gaps of 0.5 cm to the end walls. Each end space for the magnetic flux should be nearly half the cross section of a quadrant. The central parts of the both end walls are protruded to the vane ends to keep both the narrow gaps and these areas (Fig. 2.).

On the end walls, eight capacitive tuners are mounted in face of the vane ends. Through the side wall a loop tuner is inserted into each quadrant (Fig. 3.). The rf power is fed with use of a loop coupler. Each quadrant had three monitor loops.

Cooling channels are designed to surpress the thermal elongation differnce between the vanes and the tank below 100 μm at the full power of cw 25 kW. The cavity is designed to use metal vacuum sealings and is evacuated with a turbomolecular pump of 500 ℓ/s.

Electroplating The outer conductor tank is made of mild steel. The inner surface was electroplated to a thickness of 200 μm of copper using cyanide solution. The roughness is 0.4 μm. Before the vanes were assembled, the Q values were measured to inspect the quality of the plating. The measured Q value of TM010 mode was 96 % of the theoretical value for a cylindrical resonator made of pure copper.

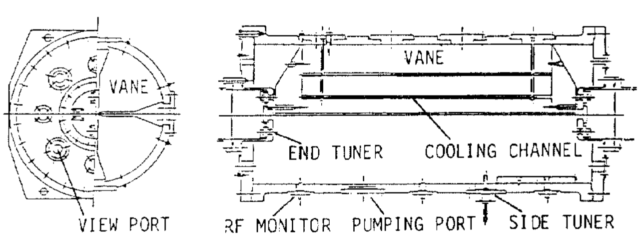

Fig. 2. Schematic drawing of the acceleration cavity of LITL.

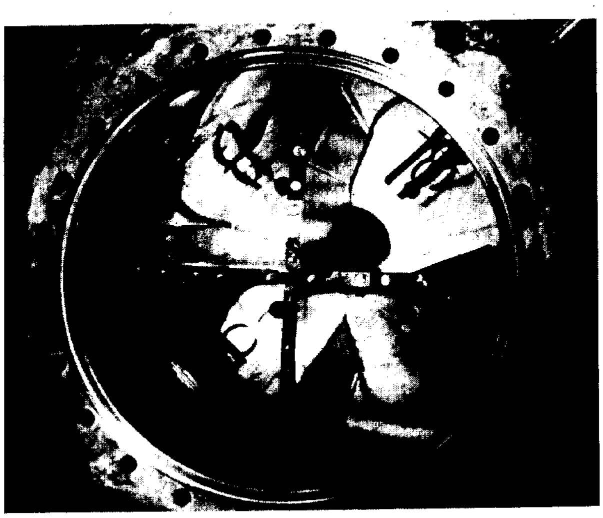

Fig. 3. The acceleration cavity of LITL.

Vane

Transverse Geometry The transverse cross section of the vane tip is approximated to a circular arc and tangential lines (Fig. 4.). The arc has a radius equal to the radius of curvature at the vane top of the theoretical shape. The model study shows that a quadrupole field is practically obtained in the acceleration bore with the shape. Also, higher intervane voltage is applicable owing to the wider intervane distance.

Modulation Machining During the manufacturing of the cold model and this cavity, the process of modulation machining was developed at Tsurumi Works, Toshiba Corporation. Sufficient accuracy was obtained in a shorter machining time.[8]

The vane is made of annealed oxygen-free copper. Before the modulation machining, cooling channels were bored into preworked vanes. The modulation was machined with a numerically controlled boring machine. A carbide ball end mill of 10 mm in diameter was used. The final cut was done at 0.5 mm longitudinal increment, after three steps of rough cuts at 2 mm increment. After the machining the surface was electropolished to a roughness of 1 ∿ 3 μm.

The modulation size was examined with a three-dimensional coordinate measuring machine. The machining error is within ± 30 μm over the vane length of 1.2 m.

Vane Assembly Each vane is attached to the tank with four base flanges (Fig. 5.). Through the flanges cooling water is supplied to the vane. The vane and the tank are contacted electrically with silver coated stainless steel tubes. The tube is 2.4 mm in diameter and silver plating is 100 μm in thickness. The vanes are assembled within an accuracy of ± 100 μm. The rectangular accuracy between adjacent vanes is within ± 1.5 mrad.

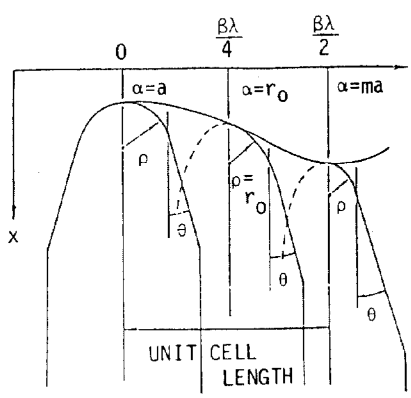

Fig. 4. Transverse cross section of the vane tip. θ = 15°.

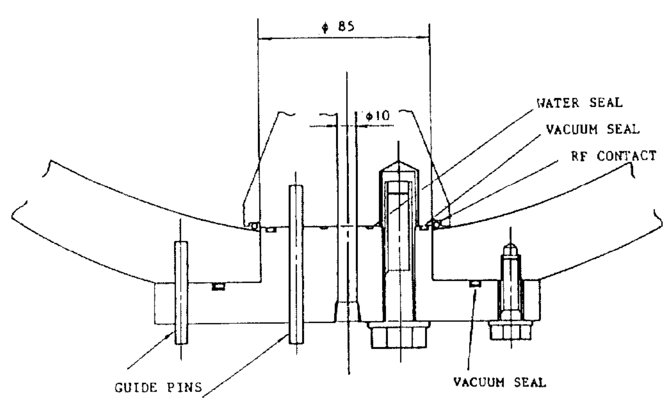

Fig. 5. Vane base flange.

Resonant Frequencies and Field Distribution

RF Characteristics

Resonant Frequencies and Field Distribution

By tuning the end capacitive turners a uniform field was attained with weak coupling. Then the tuners were readjusted slightly with coupling which matched to 50 Ω feeder line. The resonant frequency was measured as 99.6 MHz for the TE210 mode. The nearest mode was a TE110 with a resonant frequency 1.3 MHz higher. TE211 mode was found at 153.5 MHz (Fig. 6). The field distribution was measured with perturbing ball method. The obtained field uniformity is within ± 2 % azimuthally and ± 3 % longitudinally.

RF Coupling and Q Value

The unloaded Q value measured with weak coupling was 10600, 60 % of the SUPERFISH value. The reflected signal was measured for various rotating angles of the loop coupler with an area of 43 cm^2. The cavity was matched to the feeder line of 50 Ω with an effective area of 23 cm^2, which agrees with a calculated value by use of an equivalent circuit.[4]

RF Power System

The rf power is supplied with a master oscillator and power amplifier system. A tetrode tube Eimac 4CW-25000A supplies a cw rf power of 25 kW. The rf power is fed through a coaxial line WX77D to the cavity with the loop coupler. The system has a tunable width ± 10 MHz and a band width of ± 500 kHz. Both in cw and pulse operations, the rf output can be controlled by the output signal level of the master oscillator or the bias voltage of the control grid of the final tube.

Sparking Test

The intervane voltage was determined by comparing the beam test results described below with PARMTEQ simulation. In cw operation, a voltage of 62 kV was applied which corresponds to the maximum field of 205 kV/cm, or 1.8 times the Kilpatrick's criterion at 100 MHz, according to a SUPERFISH calculation. The voltage determined as described above agrees with that calculated from the measured Q value and the input rf power. In pulse operation of 20 % duty, with a duration of 5 ms and repetition period of 25 ms, 2.0 times the criterion has been achieved. The test was done in a vacuum pressure of 2×10^{-7} Torr.

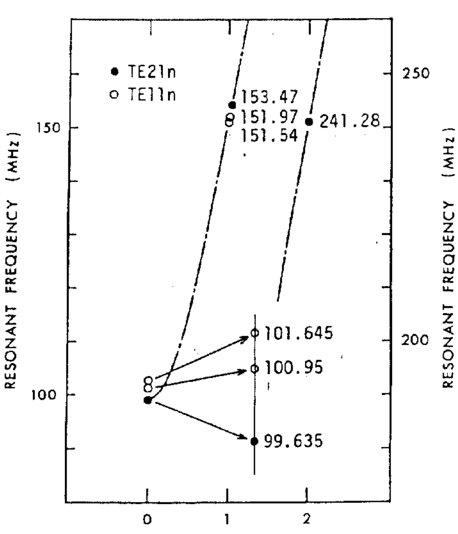

Fig. 6. Resonant frequencies of various modes.

Beam Test

Test Stand

Ion Sources A duoplasmatron type ion source was used to produce ion beams of H^+, H_2^+ and $^3He^+$. A surface ionization type ion source was used for $^7Li^+$ ions. Metallic lithium is vaporized in an oven heated at 700 °C and diffuses through a porus tungsten disk of 6 mm in diameter and 1 mm in thickness. On the hot disk surface at 1200 °C, singly charged lithium ion is produced. A few ten μA of lithium ion beam is obtained with an extraction voltage of 35 kV.

Input Beam Line The extracted ion beam at 5 keV/u is transported through two sets of einzel lenses and a separating magnet of 32 cm orbit radius and 45° bending angle. The separated ion beam is focused with a triplet of electric quadrupole lenses and an einzel lens into a phase space which matches to the RFQ acceptance (Figs. 7,8). The beam transport was designed with the computer code MAGIC. The beam intensity and emittance can be measured with a slit and Faraday cup system placed 7 cm upstream the entrance of the RFQ.

Output Beam Line The accelerated beam is focused at the object point of an analyzer magnet with a triplet of quadrupole magnets. The analyzer magnet has an orbit radius of 40 cm and a bending angle of 90°. Slit systems, multiwire profile monitors and Faraday cups are placed at the object and image points of the magnet. The momentum resolution of the analyzer system is 0.25 % in full width.

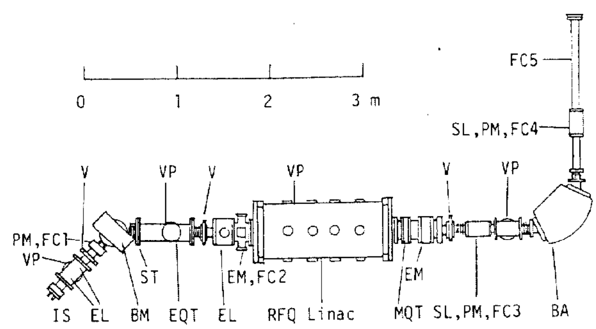

Fig. 7. Layout of the test stand.

BA	Beam Analyzer Magnet,	MQT	Mag. Q-pole Triplet
BM	Bending Magnet (45°),	PM	Profile Monitor
EL	Einzel lens,	SL	Slit System
EM	Emittance Monitor,	ST	Steering Magnet
EQT	Electric Q-pole Triplet,	V	Gate Valve
FC	Faraday Cup Monitor,	VP	Vac. Pumping Station
IS	Ion Source,		

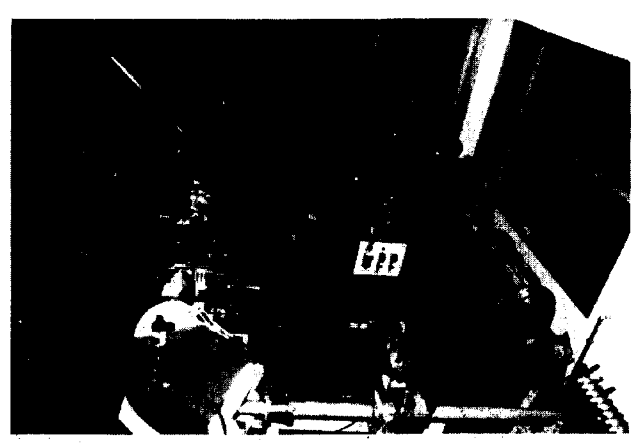

Fig. 8. View of the test stand.

Experimental Results

Beam tests have been performed by use of ion beams of H^+, H_2^+, $^3He^+$ and $^{6,7}Li^+$. Momentum spectra and output beam currents were measured as a function of the intervane voltage. The RFQ was operated in cw for H^+ and H_2^+, and in pulse mode for the others in order to apply intervane voltage higher than 62 kV. The duty factor is 35 % and pulse width is 2 ms. Injection energy is set at 5 keV/u for all the experiments. Emittances of H^+ beam were measured 7 cm upstream the RFQ, as shown in Fig. 10. The beam current is 80 μA. The X-and Y-emittance areas are 150 π and 120 π mm·mrad, respectively.

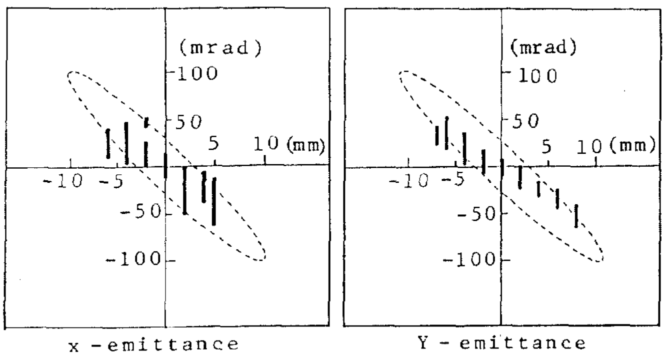

Fig. 10. Emittances of H^+ beam measured 7 cm upstream the RFQ. Beam energy is 5 keV/u. Matched phase ellipses of 300 π mm·mrad are drawn with broken lines.

Momentum Spread Momentum spectra for ion beams accelerated at the design values of the intervane voltage are shown in Figs. 11 and 12. Every peak represents the expected energy of 138 keV/u. The momentum spread is about 2 % in FWHM for each beam. Momentum spectra for various values of the intervane voltage were measured by use of H^+ beam, and are shown in Fig. 13 together with PARMTEQ results. The momentum spectrum for $V_n = 2$, where V_n is a value normalized with the design value of the intervane voltage, is 1.7 times broader than that for $V_n = 1$ in the full width and agrees well with the simulation result.

Dependence on the Intervane Voltage The output beam currents of ion beams from H^+ up to Li^+ are shown in Fig. 14 as a function of the intervane voltage. The beam currents are measured by the Faraday cup, FC3, installed 1 m downstream the magnetic quadrupole triplet. The particles which are not captured in the separatrix but transported through the RFQ can scarcely reach FC3, since the Q-triplet gives them a large divergence. Transmission for H^+ beam vs. V_n is plotted in Fig. 15. Calculated transmission with a matched beam with an emittance of 300 π mm·mrad is also shown in the figure together with transmission for non-captured beam. The experimental result shows that good transmission exceeding 90 % was achieved with V_n = 1.4 - 2.3. However, the amplitude of the transverse oscillation described approximately by Mathieu's equation increases steeply near $V_n = 3.5$ which gives a focusing strength of B = 17.5. Figure 16 represents the stability chart for the first stability region of the equation. The work line for $V_n = 3.6$ is in the unstable region through a few ten cells after the radial matching section, as shown in the figure. Both the experimental and calculated results show the output beam disappears near $V_n \approx 3.6$.

These experiments and calculations were performed with lower beam currents than the space charge limits, and satisfactory results were obtained.

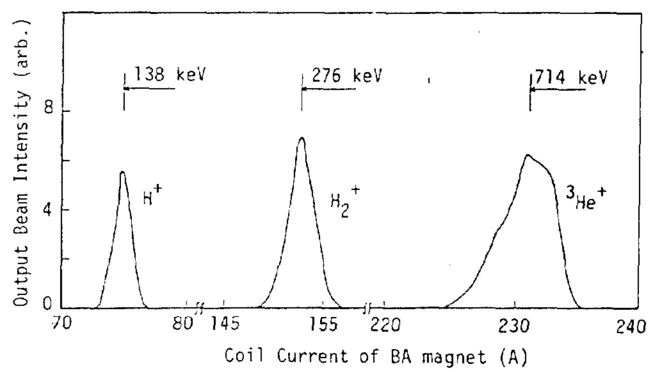

Fig. 11. Momentum spectra for H^+, H_2^+ and $^3He^+$ beams.

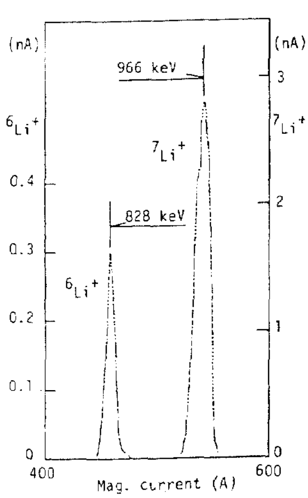

Fig. 12. Momentum spectra for $^6Li^+$ and $^7Li^+$ beams.

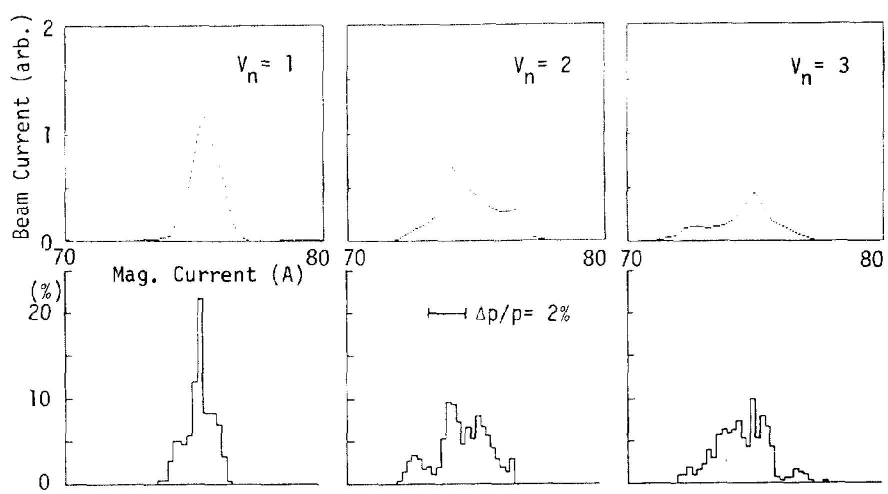

Fig. 13. Momentum spectra for H^+ beams accelerated at the various intervane voltages (upper) and PARMTEQ results (lower).

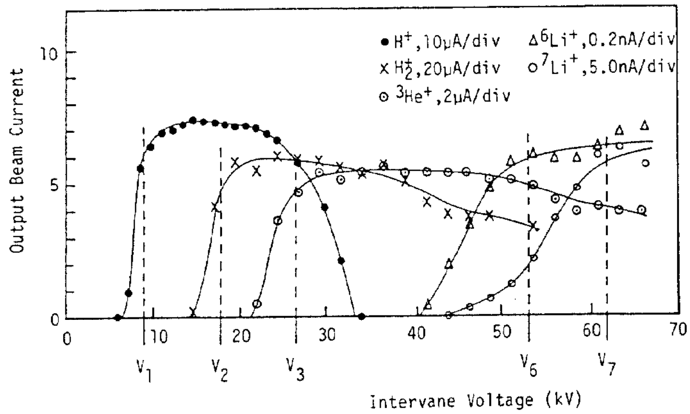

Fig. 14. Output beam currents of $H^+ \sim {}^7Li^+$ measured as a function of the intervane voltage. The design values required for each beam acceleration are indicated by $V_1 \sim V_7$.

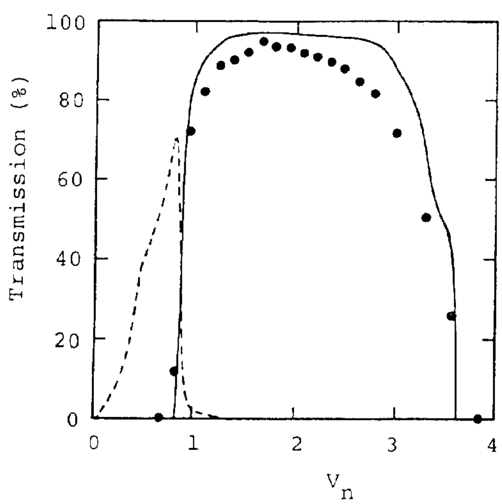

Fig. 15. Transmission for H^+ beam plotted as a function of the normalized intervane voltage. The solid line shows calculated transmission and the broken line is that for non-captured beam.

Fig. 16. RFQ stability chart. The focusing strength B and the rf defocusing strength Δ are proportional to the intervane voltage V and V·sin ϕ, respectively. The half lines show the working lines for LITL. The quantity β is related to the maximum beam size, and μ is the phase advance per focusing period.

Conclusion

Singly charged ion beam of $^7Li^+$ was accelerated sucessfully by LITL, which requires a field strength of 205 kV/cm, 1.8 times the Kilpatrick's criterion. Transmission exceeding 90 % was obtained and the acceleration characteristics agree well with the PARMTEQ simulation. The cavity is driven with a single loop coupler and frequency tuning is possible with four side inductive tuners. Operation of the machine is easy and stable. Acceleration of higher intensity beam is planned, where space charge effect will appear.

Acknowledgement

The authors thank Prof. T. Minamizono who provided kindly the lithium ion source developed at Osaka University. They also grateful to the colleague of the NUMATRON accelerator group at INS for useful discussi-ions and their helps. They thank people of Tsurumi Works, Toshiba Corporation who manufactured skillfully the LITL acceleration cavity.

References

1) I. M. Kapchinskij and V. A. Teplyakov, Prib. Tekh. Eksp., No. 2 (1970).
2) K. R. Crandall et al., Proc. 1979 Linear Acc. Conf., Montauk, NY, USA (1979) BNL-51134, 205.
3) N. Ueda et al., Proc. 1981 Linear Acc. Conf., Santa Fe, NM, USA, LA-9234-C (1982).
4) T. Nakanishi et al., INS Report NUMA-30 (1982).
5) N. Tokuda and S. Yamada, Proc. 4th Symp. Accelerator and Technology, IPCR, Wako, Saitama, Japan (1982).
6) S. Yamada, Proc. 1981 Linear Acc. Conf., Santa Fe, NM. USA, LA-9234-C (1982).
7) T. Nakanishi et al., Proc. Symp. Accelerator Aspects of Heavy Ion Fusion, GSI-82-8 (1982).
8) S. Itoh et al., INS Report, NUMA-51, to be published.